

# *Identification of Cracks In Functionally Graded Material Beams Using the H-Version of Finite Element Method*

Narimane Hassaine<sup>1</sup> \*, Ahmed Fellah<sup>2</sup>

<sup>1</sup>LTI, Laboratoire des Technologies Innovantes, Ecole Nationale Supérieure de Technologie Avance, Ex Biomedical, Derganna, Algeria.

<sup>2</sup>IS2M Laboratory, Department of Mechanical Engineering, Faculty of Technology, University of Tlemcen, Tlemcen, Algeria.

\*Corresponding author; Email: [narimane.hassaine@enst.dz](mailto:narimane.hassaine@enst.dz).

---

## Article Info

### *Article history:*

Received 13/04/ 2023

Revised 29/04/ 2023

Accepted 25/05/2023

---

### *Keywords:*

FG beam  
natural frequency  
crack  
h- Version method

---

---

## ABSTRACT

In this article, we analyze the effect of transverse cracks on the natural frequencies of a Euler-Bernoulli functional gradient beam. The studied beam was discretized into finite elements and the global matrices of the motion equation are determined by applying the Lagrange equation to the beam kinetic and deformation energies. The material properties are considered to vary in the directions of the beam thickness, the gradation is described by the power-law distribution, the stiffness of the cracked element is determined based on the reduction of the beam cross-section. The numerical results obtained are compared with those available in the previous study. Finally, case studies were carried out to analyse the influence of the power law index, the depth and the opposition of the crack on the natural frequencies of the beam for different boundary conditions; these studies demonstrate the advantage of the FGM beam over the purely metal beam.

---

## I. INTRODUCTION

The FGM concept first appeared in Japan in 1984 as a suggested thermal barrier material capable of withstanding a surface temperature of 2000 K and a temperature gradient of 1000 K across a cross-section  $< 1mm$  [1]. In recent years, functionally graded materials (FGM) have been considered as one of the advanced inhomogeneous composite materials with great application potential in many high temperatures engineering fields such as aerospace vehicles, nuclear reactors, power generators, automotive industries. FGMs typically consist of a continuously gradient mixture of metals and ceramics in the compositional profile, so they can take advantage of the heat and corrosion resistance of ceramics and the mechanical toughness of metals, while reducing the extent of residual and thermal stresses.

Cracks frequently appear in FG structures, which pose a serious threat to the safety of their performance. Many research efforts have been devoted to the analysis of the failure of FGMs with different configurations [2-4]. However, the early detection of cracks in FGM structures is necessary to prevent possible catastrophic failure.

The presences of a crack in a structure will influence its stiffness and damping properties and change its vibrational characteristics, which can be measured and employed to detect and quantify the crack. Vibration-based inspection approaches have received considerable attention over the past three decades. There is a large body of literature that studies crack modeling, free and forced vibration, and crack diagnosis. Chondros and Dimarogonas [5] provided a detailed overview of approaches to predict the change in dynamic characteristics as function of crack location and size. Dimarogonas [6] reviewed analytical, numerical, and experimental studies on crack recognition based on dynamic feature changes. Doebling et al [7] reviewed methods for detecting, locating, and estimating the

severity of damage in structural systems by examining changes in measured vibration responses.

Depending on the loading conditions and vibration amplitude, crack models are generally divided into two categories: the open and the breathing model [8]. In the open model, the crack is always open during vibration, while it alternately opens and closes in the breathing model. The open crack model mainly includes an equivalent linear spring or local flexibility connecting the two segments of the beam, a local change in the modulus of elasticity, reduced cross sections, and a continuous variation of the flexibility along the length of the beam. A breathing crack, usually simulated by a bilinear spring, can produce interesting and complicated nonlinear dynamic behavior. Most previous research uses the open crack model while comparatively few studies have been conducted applying the breathing crack model. Narkis [9] simulated the cracks as an equivalent rotating spring and studied the dynamics and identification problems of a uniform cracked, simply supported beam. Dado [10] reported a comprehensive crack identification algorithm for beams under different support conditions using the local flexibility approach. Christides and Barr [11] developed a one-dimensional continuous Euler-Bernoulli beam theory cracked by the generalized variational principle and an assumed crack perturbation function to be determined by experiments. Yang et al [12] proposed an expression for the continuously varying bending stiffness of beams with open crack based on the energy method. Chondros et al [8] used a bilinear crack model and the vibration theory of continuously cracked beams to predict changes in the transverse vibration of a simply supported beam with an open crack. It should be noted that these crack models must be properly applied taking into account the assumptions under which the models were derived or valid, otherwise incorrect conclusions would be drawn.

In this study, we used the traditional finite element approach to examine the dynamic behavior of a functionally graded beam (h-FEM). The beam is discretised into finite elements Euler-Bernoulli beam and the global equation of motion is obtained applying the Lagrange's equation taking into account the variation of the stiffness of the cracked element. According to the power law distribution, the material properties are considered graded in the thickness directions of the beam. The natural frequencies are determined numerically using a program developed in MATLAB, the obtained results are verified with those reported in literature for FG beam. Finally, The purpose of case studies is to illustrate the benefits of FGM and pure metallic models by showing how the power law index, the depth, and the position of the fracture affect the natural frequencies of the beam.

## II. MATERIALS AND METHOD

Consider a beam with a length  $L$ , width  $b$ , and thickness  $h$ ; which is composed of a metallic core and covered with ceramic as seen in Fig. 1. In our study, the material properties  $P$  of the beam vary continuously along the thickness ( $z$  axis) according to the following relation:

$$P(z) = P_1 V_1(z) + P_2 V_2(z) \quad (1)$$

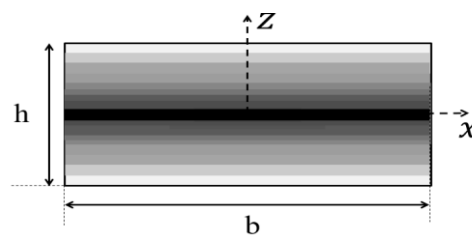


Figure 1. Schematic of FG beam

Where  $P(z)$  denotes either the density or the Young's modulus  $E(z)$ .  $V_1(z)$  and  $V_2(z)$  are the volume fractions of the metal and ceramic components, fulfilling the following relation

$$V_1(z) + V_2(z) = 1 \quad (2)$$

$$P(z) = (P_2 - P_1) \left( 1 - \left( \left| \frac{2z}{h} \right| - 1 \right) \right)^n + P_1 \quad (3)$$

Where:

$n$ : represents the power index of the material's gradation along the  $z$  axis (thickness direction).

From this relation, we can deduce several cases:

- $n = 0$ : the material properties vary only in the thickness direction (along the  $z$  axis).
- $n = \infty$ : denotes a pure ceramic beam ( $V_1(x, z) = 0$ ).
- $n = 0$ : denotes a pure metallic beam ( $V_1(x, z) = 1$ ).
- $n = 1$ : denotes a linear gradation.

For an element of length  $L_e$ , the expression of the kinetic energy  $E_c$  and the strain energy  $E_p$  of the FG beam are given by

$$E_c = 1/2 \int_0^{L_e} A_{11} \dot{w}^2 dy \tag{4}$$

$$E_p = 1/2 \int_0^{L_e} B_{11} \left( \frac{\partial^2 w}{\partial y^2} \right)^2 dy \tag{5}$$

Where  $w$  represent the transverse displacement along the  $z$ -axis; the expression of  $A_{11}$  and  $B_{11}$  are given as:

$$A_{11} = \int_s \rho(z) ds = b \int_{-h/2}^{h/2} \rho(z) dx dz \tag{6}$$

$$B_{11} = \int_s E(z) z^2 ds = b \int_{-h/2}^{h/2} E(z) z^2 dx dz \tag{7}$$

According to the Eq.4, The Young's modulus  $E(x, z)$  and mass density  $\rho(x, z)$  are given as:

$$\rho(z) = (\rho_2 - \rho_1) \left( 1 - \left( \left| \frac{2z}{h} \right| - 1 \right) \right)^n + \rho_1 \tag{8}$$

$$E(z) = (E_2 - E_1) \left( 1 - \left( \left| \frac{2z}{h} \right| - 1 \right) \right)^n + E_1 \tag{9}$$

### II.1. Finite element method

Beam was discretised into 10 elements with two degree of freedom of one element, as shown in Fig. 2, the transverse displacement  $w$  is replaced with the vector of shape functions  $N_w$  [13] and the vector of generalized coordinates  $q_w$ .

$$w = [N_w] \{q_w\} \tag{10}$$

While the expression of the kinetic energy  $E_c$  and the strain energy  $E_p$  of the FG beam will be:

$$E_c = 1/2 \int_0^{L_e} A_{11} \{\dot{q}_w\}^t \{N_w\}^t \{N_w\} \{\dot{q}_w\} dy \tag{11}$$

$$E_p = 1/2 \int_0^{L_e} B_{11} \{q_w\}^t \{N_w''\}^t \{N_w''\} \{q_w\} dy \tag{12}$$

### II.2. Modelling of cracked elements

In fig. 2,  $L_c$  represent the crack location from the left end of the beam and  $a$  is the depth of the crack, the non-dimensional parameters of the crack are given as:

$$\begin{cases} \bar{l} = \frac{L_c}{L} \\ \bar{h} = \frac{2a}{h} \end{cases} \tag{13}$$

The previous studies on the cracked beams denote that the cracks reduced its stiffness, in our study, the reduce of the beam's stiffness will translated by the reduction of the cross-section of the beam due to the crack depth propagation as shown in Fig. 2. In this case, the expression of the coefficient  $B_{11}$  is given as:

$$B_{11\ crack} = b \int_{-h/2}^{(h/2-a)} E(z) Z^2 dz \tag{14}$$

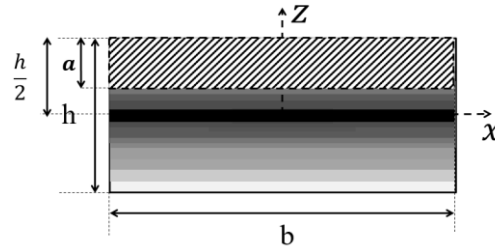


Figure 2. Cross section of the cracked element

### II.3. Total Equation of Movement

The elementary masse [Me] and stiffness matrices of uncracked [Ke] and cracked [Kec] element of the studied beam are developed by the application of Lagrange's equation.

$$\frac{d}{dt} \left( \frac{\partial E_C}{\partial \dot{q}_w} \right) + \frac{\partial E_p}{\partial q_w} = 0 \tag{15}$$

Where:

$$[M_e] = A_{11} \int_0^{Le} \{N_w\}^t \{N_w\} dy \tag{16}$$

$$[K_e] = B_{11} \int_0^{Le} \{N_w''\}^t \{N_w''\} dy \tag{17}$$

$$[K_{ec}] = B_{11\ crack} \int_0^{Le} \{N_w''\}^t \{N_w''\} dy \tag{18}$$

The assembly of previous matrices taking into account the location of the cracked element allow us to determine the global masse [M] and stiffness [K] matrices of the governing equation of motion.

$$[M]\{\ddot{q}_w\} + [K]\{q_w\} = 0 \tag{19}$$

The natural frequencies are obtained from the eigen solution of the equation given as:

$$|[K] - \omega^2[M]| = 0 \tag{20}$$

### II.4. Validation

In order to validate the developed FE model for cracked FG beam and given the lack of studies on this model, we choose to compare our results in the case of uncracked FG cantilever beam with those given by Piovan et al [14] where the material gradation vary in the thickness direction , the geometric and material characteristic of the beam are given in table.1.

Fig. 4 illustrates the comparison between the obtained natural frequencies of first three modes of the cantilever beam compared with Piovan et el [14]. The obtained results are in an excellent agreement with the results of Piovan et el [14] .

Table 1. Geometric and material properties of FG beam.

Geometric properties
----------------------

Length	$L = 1\text{ m}$	Width	$b = 0.01\text{ m}$	Thickness	$h = 0.02\text{ m}$
Material properties					
	Steel (metal)		Alumina $\text{Al}_2\text{O}_3$ (ceramic)		
Young's modulus $E$ [GPa]	2,14		3,9		
Mass density $\rho$ [ $\text{Kg.m}^{-3}$ ]	7800		3200		

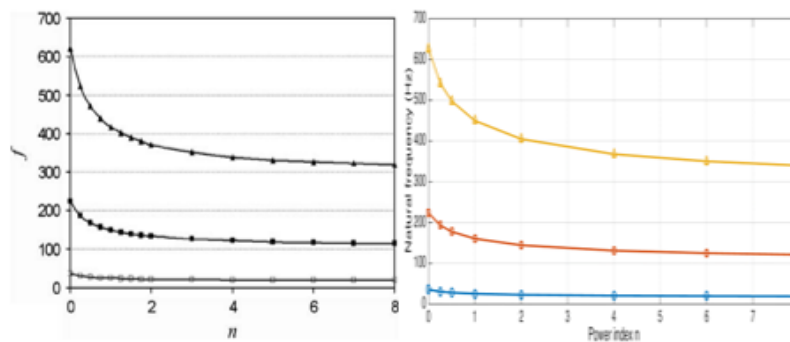


Figure 4. Validation of the natural frequencies of the first three modes.

### III. RESULTS

In this section, several case studies were conducted to analyse the influence of power law index, depth and crack location on the natural frequencies of the beam for different boundary conditions; the geometric and material parameters of the beam are given in table 1.

These studies demonstrate the advantage of the model of FG beam and the metallic models.

Table 2 represents the variation of the natural frequencies of the first three modes of vibration for uncracked FG beam as function to the power index for different boundary conditions. From the results of this table, we can see that the natural frequencies of FG beam are comprised between the natural frequencies of pure ceramic and pure metallic beam. For the same value of power index; the frequencies of FG beam approach to the pure metallic more than the FG beam; that mean the characteristics (lower elastic modulus and higher density) of bi-directional model are more close to the pure metallic more than the unidirectional model.

The effect of the crack depth  $\bar{h}$  and crack location  $\bar{l}$  on the natural frequencies of pure metallic and FG beams is shown in tables 3 and 5.

The frequency's decrease is more important in the case of cantilever beam compared to the simply supported and clamped beams for the two models.

In the case of cantilever beams, the severity of crack's location increase when the crack approach to the fixed side for the first and second modes, for the third mode, it increase when the crack approach to the middle. In the case of Simply Supported and Clamped-Clamped beams, it increase when the crack approach to the middle.

Table 2. Natural frequencies of the uncracked beam according to the power law index for different boundary conditions.

Power index	Natural frequencies (Hz)		
	FG beam		
	$F_1$	$F_2$	$F_3$
	Cantilever beam		
0 (pure ceramic)	35.7	223.5	626
0.25	30.88	193.55	542.06
1	25.62	160.6	449.77
4	20.95	131.33	367.80
10	18.97	118.92	333.04
20	18.06	113.20	317.04
$\infty$ (pure metallic)	16.92	106.06	297.03
Simply Supported beam			
0 (pure ceramic)	100.12	400.52	901.55
0.25	86.69	346.8	780.63
1	71.93	287.75	647.72
4	58.82	235.31	529.68
10	53.26	213.07	479.62
20	50.70	202.83	456.57
$\infty$ (pure metallic)	47.50	190.03	427.75
Clamped-Clamped beam			
0 (pure ceramic)	226.97	625.78	1227.7
0.25	196.52	541.85	1063.0
1	163.07	449.6	882.03
4	133.35	367.66	721.28
10	120.74	332.91	653.11
20	114.94	316.91	621.73
$\infty$ (pure metallic)	107.68	296.91	582.48

Table 3. Influence of the crack depth on the natural frequencies of the FGM beam for different boundary conditions where  $\bar{\Gamma}=0.15$

Non-dimensional crack depth $\bar{h}$	Natural frequencies (Hz)					
	Pure metallic beam (n = $\infty$ )			FG beam (n = 2)		
	$F_1$	$F_2$	$F_3$	$F_1$	$F_2$	$F_3$
	Cantilever beam					
0	16.92	106.06	297.03	23.07	144.59	404.96
0.25	16.11	105.25	295.98	21.81	143.34	403.33

0.5	15.47	104.63	295.06	20.98	142.54	402.11
0.75	15.16	104.34	294.59	20.65	142.24	401.60
1	15.11	104.2	294.1	20.6	142.2	401.5
Simply Supported beam						
0	47.50	190.03	427.75	64.8	259.1	583.2
0.25	47.09	185.22	413.46	64.1	251.6	561
0.5	46.73	181.12	402.71	63.65	246.22	547.28
0.75	46.55	179.12	397.89	63.45	244.09	542.17
1	46.52	178.81	397.15	63.42	243.79	541.48
Clamped-Clamped beam						
0	107.68	296.91	582.48	146.8	404.8	794.2
0.25	106.77	295.85	573.81	145.4	403.2	780.7
0.5	106.07	294.92	566.98	144.5	401.9	771.9
0.75	105.75	294.44	563.80	144.2	401.4	768.5
1	105.7	294.3	563.3	144	401.3	768.0

Table 4. Influence of the crack location on the natural frequencies of the FGM beam for different boundary conditions where  $\bar{h} = 0.35$

Non-dimensional crack location $\bar{l}$	Natural frequencies (Hz)					
	Pure metallic beam ( $n = \infty$ )			FG beam ( $n = 2$ )		
	$F_1$	$F_2$	$F_3$	$F_1$	$F_2$	$F_3$
Cantilever beam						
0.15	15.82	104.96	295.57	21.41	142.95	402.76
0.25	16.14	105.71	287.34	21.89	144.07	390.40
0.35	16.41	103.59	286.50	22.29	140.87	389.20
0.55	16.76	100.50	293.87	22.83	136.22	400.21
0.85	16.91	105.56	290.58	23.06	143.85	395.14
Simply Supported beam						
0.15	46.93	183.39	408.51	63.90	249.03	554.33
0.25	46.19	180.75	417.66	62.8	245.1	568.1
0.35	45.49	183.91	425.57	61.72	249.90	579.88
0.55	45.08	188.81	411.97	61.1	257.2	559.5
0.85	46.93	183.39	408.51	63.90	249.03	554.33
Clamped-Clamped beam						
0.15	106.5	295.4	570.7	145.	402.6	776.4
0.25	107.4	287.1	563.6	146.	390.1	766.1
0.35	105.74	286.15	579.37	143.9	388.7	789.4

0.55	103.98	294.28	562.89	141.2	400.9	764.8
0.85	106.45	295.44	295.44	145.0	402.6	776.4

#### IV. CONCLUSION

In the present paper, a finite element model is developed for a functionally graded beam using the Euler-Bernoulli beam theory. Various analyses are carried out to evaluate the influence of crack depth and location on the natural frequencies of a pure metallic and FG beams, the obtained results show that:

- The natural frequencies of FG beam are comprised between the natural frequencies of pure ceramic and pure metallic beam.
- The natural frequencies decrease when the crack depth increases for the different studied model.
- The crack depth and location had an important effect on the stiffness of the FG beam compared to Pure metallic beam.

#### References

- [1] Chen, X.L, Liew, K.M (2004). Buckling of rectangular functionally graded material plates subjected to nonlinearly distributed in-plane edge loads, *Smart Mater. Struct.* 13 1430–1437.
- [2] Ayhan, A.O (2007). Stress intensity factors for three-dimensional cracks in functionally graded materials using enriched finite elements, *International Journal of Solids and Structures* 44 8579–8599.
- [3] GU, P, Asaro, R.J (1997). Cracks in functionally graded materials, *International Journal of Solids and Structures* 34 1–17.
- [4] Cheng, Z., Zhong, Z (2006). Fracture analysis of a functionally graded strip under plane deformation, *Acta Mechanica Solida Sinica* 19.
- [5] Chondros, T.G, Dimarogonas A.D (1989). Dynamic sensitivity of structures to cracks, *Journal of Vibration, Acoustics, Stress and Reliability in Design* 111 251–256.
- [6] Dimarogonas, A.D (1996). Vibration of cracked structures: a state of the art review, *Engineering Fracture Mechanics* 55 831–857.
- [7] S.W. Doebling, C.R. Farrar, M.B. Prime, D.W. Shevitz, A review of damage identification methods that examine changes in dynamic properties, *Shock and Vibration Digest* 30 (1998) 91–105.
- [8] Chondros, T.G., Dimarogonas, A.D., Yao, J. (2001). Vibration of a beam with a breathing crack, *Journal of Sound and Vibration* 239 (1) 57–67.
- [9] Narkis, Y (1994). Identification of crack location in vibrating simply supported beams, *Journal of Sound and Vibration* 172 (4) 549–558.
- [10] Dado, M.H (1997). A comprehensive crack identification algorithm for beams under different end conditions, *Applied Acoustics* 51 (4) 381–398.
- [11] Christides, S., Barr, A.D.S (1984). One-dimensional theory of cracked Bernoulli–Euler beams, *International Journal of Mechanical Sciences* 26 639–648.
- [12] Yang, X.F., Swamidias, A.S.J. R. Seshadri (2001). Crack identification in vibrating beams using the energy method, *Journal of Sound and Vibration* 244 (2) 339–357.
- [13] Bardell, N.S (1996) .“An engineering application of the h-p version of the finite element method to the static analysis of a Euler-bernoulli beam”. *Computers & Structures*, 59(2), 195-211
- [14] M.T. Piovan a, R. Sampaio, (2009). A study on the dynamics of rotating beams with functionally graded properties, *Journal of Sound and Vibration*. 327, (1–2), 134-143. DOI:10.1016/j.jsv.2009.06.015